Available online at www.sciencedirect.com
ScienceDirect
International Journal of Multiphase Flow 33 (2007) 691–706
International Journal of Multiphase Flow
www.elsevier.com/locate/ijmulflow

Experimental studies on CHF characteristics of nano-fluids at pool boiling

Hyung Dae Kim [a], Jeongbae Kim [b], Moo Hwan Kim [a,*]

[a] Department of Mechanical Engineering, Pohang University of Science and Technology, San 31, Hyoja-dong, Namgu, Pohang, Kyoungbuk 790-784, Republic of Korea
[b] Korea Institute of Energy Research, Jang-dong, Yuseong-gu, Daejeon, 305-343, Republic of Korea

Received 24 May 2006; received in revised form 19 February 2007

Abstract

To investigate the CHF characteristics of nano-fluids, pool boiling experiments of nano-fluids with various concentrations of TiO_2 or Al_2O_3 nanoparticles were carried out using a 0.2 mm diameter cylindrical Ni–Cr wire under atmospheric pressure. The results show that the CHFs of various nano-fluids are significantly enhanced over that of pure water. SEM observation subsequent to the CHF experiment revealed that a nanoparticle coating is generated on the wire surface during pool boiling of nano-fluids. The CHF of pure water was measured on a nanoparticle-coated wire which was produced during the pool boiling experiments of nano-fluids. The CHF of pure water on the nanoparticle-coated wire was similar to that of nano-fluids. This result clearly shows that the main reason for CHF enhancement of nano-fluids is the modification of the heating surface by the nanoparticle deposition. The nanoparticle-coated surface was characterized with various parameters closely related to pool boiling CHF: surface roughness, contact angle, and capillary wicking performance. Finally, CHF enhancement of nano-fluids is discussed using the parameters.

Keywords: Capillary wicking; CHF; Contact angle; Nano-fluids; Nanoparticle surface coating; Surface roughness

1. Introduction

Critical heat flux (CHF) in pool boiling is an undesirable phenomenon causing an excessive increase of the temperature at the boiling surface. Such a tremendous increase of temperature can lead to a fatal crisis in various thermal systems, such as boilers and nuclear reactor systems. Therefore, enhancing the CHF will provide the thermal system with a greater safety margin. Typical approaches to enhance CHF include: vibration of the surface or fluid to promote bubble departure from the heating surface; coating with porous media to increase

* Corresponding author. Tel.: +82 54 279 2165; fax: +82 54 279 3199.
E-mail address: mhkim@postech.ac.kr (M.H. Kim).

0301-9322/$ - see front matter © 2007 Elsevier Ltd. All rights reserved.
doi:10.1016/j.ijmultiphaseflow.2007.02.007

the number of active cavities and to improve the supply of cooling liquid to the heating surface; applying an electric field to promote the departure of bubble from heating surface.

In addition to the conventional methods for CHF enhancement, You et al. (2003) introduced a new approach to enhance pool boiling CHF using 'nano-fluids', a new kind of heat transfer fluid in which nanoparticles are uniformly and stably dispersed. They performed pool boiling experiments with a $1 \times 1\ cm^2$ polished copper surface immersed in water–Al_2O_3 nano-fluids under the pressure of 19.94 kPa (the saturation temperature for that pressure was about 60 °C). The concentrations of nanoparticles were ranged from 0 g/l to 0.05 g/l. The pool boiling curves of those nano-fluids demonstrated that the CHF could be increased dramatically (about three times as high as the CHF of pure water). However, they concluded that the unusual CHF enhancement could not be explained by any existing CHF model.

Vassallo et al. (2004) studied the pool boiling heat transfer characteristics of 0.5% solutions of silica particles with diameters from 15 to 3000 nm. Pool boiling experiments were carried out using a 0.4 mm diameter Ni–Cr wire at atmospheric pressure. The results showed a considerable increase in the CHFs of both nano- and micro-solutions compared to water. At the end of the tests, a silica coating (about 0.15–0.2 mm thick) was observed on the wire, indicating some possible surface interaction between the nano solution and the wire at higher heat fluxes.

Bang and Chang (2005) performed pool boiling experiments on nano-fluids with volume concentrations from 0% to 4% of alumina nanoparticles using a smooth horizontal flat surface under atmospheric pressure. The results showed that the CHF of nano-fluids could be enhanced in not only horizontal but also vertical heating conditions. From the roughness change of the heating surface before and after experiments, they hypothesized that CHF characteristics might change due to the coating of heating surface with nanoparticles, but could not reveal the exact reason.

Milinova and Kumar (2005) studied pool boiling heat transfer of pure and silica nano-fluids using a 0.32 mm diameter electrically heated Ni–Cr wire at atmospheric pressure. Two characteristics of silica nanoparticles were explored: one is the role of the salts and the other is the effect of particle size on CHF. They distinctly showed the significant deposition of silica on the heater surface using SEM observation. They also conjectured that the surface porosity is responsible for increasing heat transfer.

Recently, Kim et al. (2006a) carried out an experimental study to show the effect of nanoparticle surface coating on the abnormal CHF enhancement using nano-fluids. They conducted a pool boiling CHF test of water–TiO_2 nano-fluids using horizontally suspended thin wire heater. SEM observation of the heater surface subsequent to the test revealed the serious coating of nanoparticles on the heating surface during the pool boiling of nano-fluids. In addition, CHF of pure water on the nanoparticle-coated heater sufficiently reproduced CHF of nano-fluids. The result clearly showed that the main cause of CHF enhancement of nano-fluids was the change of surface properties of the heater due to the nanoparticle surface coating formed during pool boiling. Subsequently, Kim et al. (2006b) confirmed with an experimental study analogous to Kim et al. (2006a) that the CHF enhancement in nano-fluids appears to correlate with the presence of a layer of nanoparticles that build up on the heated surface during nucleate boiling. However, both still could not elucidate the mechanism of CHF enhancement on the surface without quantitative characterization of the heating surface.

In this work, we attempted to extensively investigate pool boiling CHF characteristics of nano-fluids as well as to relate the parameters governing CHF phenomena with the unusual CHF enhancement of nano-fluids. In this regard, two experimental works were performed, one is a pool boiling CHF experiment and the other is the characterization of the heating surface modification occurring in the experiments.

Pool boiling experiments of nano-fluids are carried out for nano-fluids with volumetric particle concentrations from 10^{-5}% to 10^{-1}% using TiO_2 and Al_2O_3 nanoparticles and 0.2 mm diameter Ni–Cr wire. Since a careful review of previous research shows that the CHF enhancement of nano-fluids is closely related to the modification of the heating surface by nanoparticles, the wire surface subsequent to pool boiling of nano-fluids is examined using scanning electron microscope (SEM). And the effect of the modified wire surface on CHF is also experimentally investigated.

The wire surface is characterized using surface parameters relevant to CHF: surface roughness, contact angle, and capillary wicking performance. The reason for CHF enhancement of nano-fluids is discussed using those surface parameters in detail.

2. Pool boiling experiment

2.1. Preparation and characterization of nano-fluids

In this work, nano-fluids were prepared by the two-step method, dispersing dry nanoparticles into the base liquid. Distilled water was used as a base liquid, and Al_2O_3 and TiO_2 nanoparticles were used. The nanoparticles were manufactured by the patented physical vapor synthesis (PVS) process of Nanophase Technologies Corporation and by the sol–gel process of Advanced Nano Product Corporation, respectively. Some additives (dispersants or surfactants) could have been used to stabilize the nanoparticle suspensions, but the additives could exert a significant influence on the rheological behavior of the fluids and the boiling heat transfer (Wen and Ding, 2005). Therefore, in this work, no additive was used and ultrasonic excitation was performed for 3 h just before pool boiling experiments. Nanoparticles dispersed without other additives do not change the surface tension of the base fluid (Das et al., 2003).

The characteristics of nano-fluids are governed by not only the kind and size of the nanoparticles but also their dispersion status in the base fluid. Fig. 1 shows nanoparticles dispersed in distilled water. The Al_2O_3 nanoparticles were spheres with a mean diameter of 47 nm and a range from 10 to 100 nm, as estimated from TEM images. On the other hand, the TiO_2 particles had polygonal morphology, with a mean particle size of 23 nm and a deviation of only about 10 nm. However, the nanoparticles dispersed with no additive might have the weak electrostatic repulsion between themselves and be easily agglomerated in the colloidal state. Nanoparticle aggregation actually occurred in both nano-fluids without additive. Aggregated nanoparticles made an irregular cluster. In particular, the aggregation of TiO_2 nanoparticles was more serious.

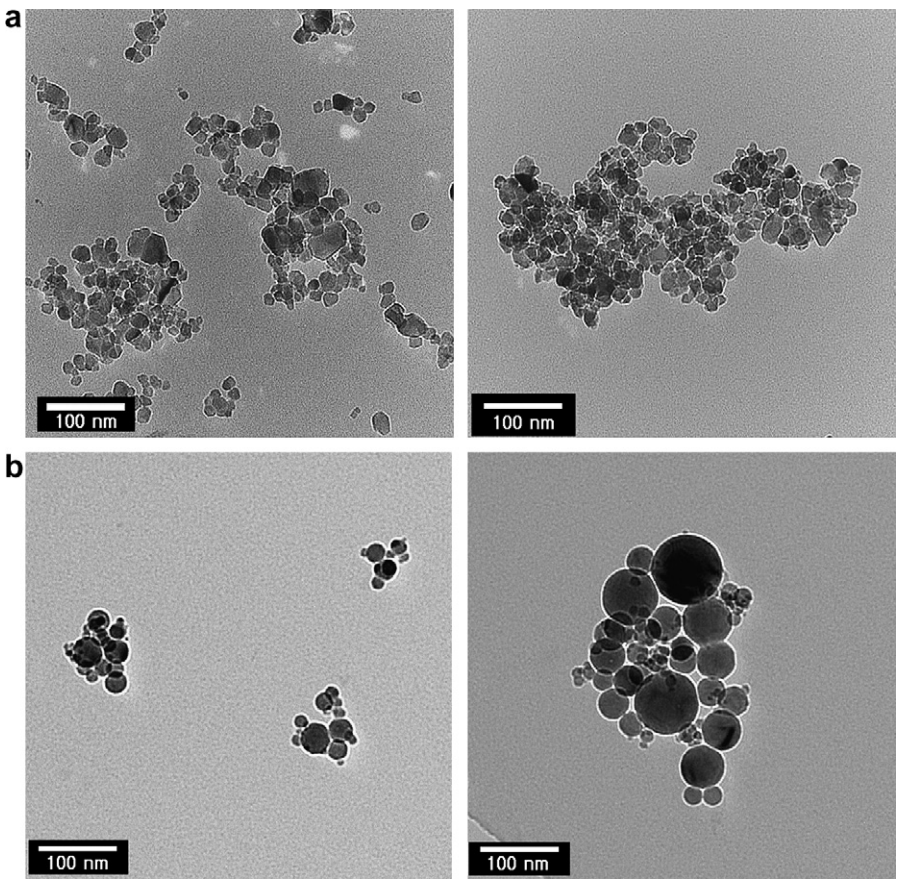

Fig. 1. TEM images dispersed in distilled water: (a) TiO_2; (b) Al_2O_3.

The amount of nanoparticles dispersed in the solution was quantified not by mass concentration but by volume concentration, because it is known that the flow phenomenon of a liquid–solid solution depends on the hydrodynamic force acting upon the surface of solid particles. But, as it is very difficult to directly measure the precise true volume of nanoparticles, the following conversion formula is conventionally used to calculate the volume concentration (ϕ_V) of nanoparticles in nano-fluids (Bang and Chang, 2005):

$$\phi_V = \frac{1}{\left(\frac{1-\phi_m}{\phi_m}\right)\frac{\rho_p}{\rho_f} + 1} \tag{1}$$

where ϕ_m is the mass concentration of nanoparticles, ρ_f is the liquid density, and ρ_p is the nanoparticle density. Five different volume concentrations were prepared ranging from 10^{-5}% to 10^{-1}%.

The thermal conductivity enhancement is a very important physical property of nano-fluids as a cooling fluid. However, the volume concentrations in the present work were too low to expect a considerable enhancement of thermal conductivity (Murshed et al., 2005). Due to the same reason, the viscosity and density also had nominal changes (Brinkman, 1951).

2.2. Experimental procedure and uncertainty

A schematic diagram of the experimental apparatus is shown in Fig. 2. The main test pool consists of a 250 mm × 140 mm × 250 mm rectangular Pyrex glass vessel and a 30 mm thick Teflon cover. The simple geometry and glass material of the test chamber ensured that clean conditions could be maintained for each experiment. The working fluid was pre-heated using a Corning hot plate and the pool temperature was measured with a Pt-100 ohm RTD sensor. The reflux condenser cooled with tap water prevented the loss of vapor from the test chamber. Accordingly, the volume concentration of the working fluid did not change during the experiments. The opening on the top of the condenser maintained the system pressure at atmospheric pressure.

The heating material was a horizontally suspended Ni–Cr wire ($d = 0.2$ mm). Since the wire is commercially mass-produced, the surface conditions of all test wires were uniform. After each pool boiling CHF experiment,

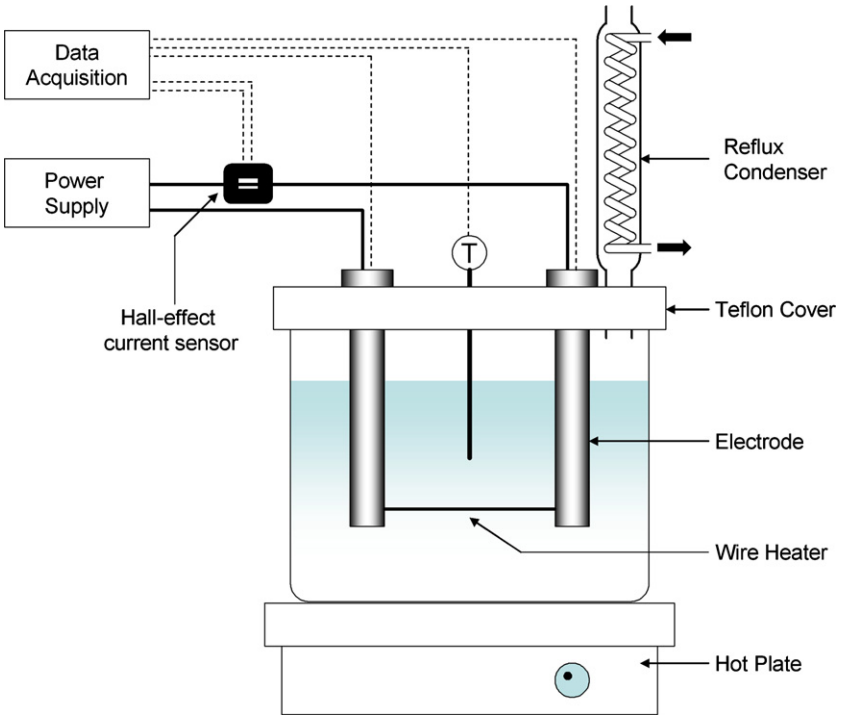

Fig. 2. Schematic diagram of the experimental apparatus for pool boiling.

the wire was examined using scanning electron microscope (SEM) to identify the deposition of nanoparticles on the wire surface.

The ends of the wire were clamped to 10 mm diameter cylindrical copper electrodes. The electrodes were connected to a HP agilent 6575A DC power supply (120 V/18 A). A LEM hall-effect current sensor was used to measure the current. An HP agilent 34970A data acquisition system was used to measure and store voltage, current, and temperature data.

All pool boiling experiments were started after the bulk temperature of the working fluid was steadily maintained at the saturated temperature. Increasing electric power was supplied to the wire. As the heat flux neared the CHF, the power was increased in smaller increments. At the CHF, the resistance of the wire increased sharply, resulting in an instantaneous breakage of the wire. The CHF ($\dot{q}''_{CHF}$) was calculated using data obtained immediately before the steep increase of wire resistance:

$$\dot{q}''_{CHF} = V_{max} I_{max} / \pi D L \tag{2}$$

Here, V_{max} is the voltage drop and I_{max} is current at the CHF point, D is the wire diameter, and L is the wire length.

The experimental uncertainty using the method proposed by Holman (2001) is represented as follows:

$$\frac{U_{\dot{q}''_{CHF}}}{\dot{q}''_{CHF}} = \sqrt{\left(\frac{U_{V_{max}}}{V_{max}}\right)^2 + \left(\frac{U_{I_{max}}}{I_{max}}\right)^2 + \left(\frac{U_D}{D}\right)^2 + \left(\frac{U_L}{L}\right)^2} \tag{3}$$

The main sources of uncertainty to be considered are the applied voltage and the length of wire. There is also the contact resistance between the wire and the copper electrodes because they are connected by only mechanical clamping. The uncertainties of the applied voltage and the length of wire are estimated to be less than $\pm 4.0\%$ and $\pm 1.7\%$, respectively. From the above analysis, the maximum uncertainty at the pool boiling CHF is estimated at $\pm 4.4\%$.

2.3. Experimental cases

A careful review of previous research on boiling of nano-fluids suggested that nanoparticles would deposit on the heating surface during pool boiling of nano-fluids. Thus, the effect of nanoparticles on CHF should consider two topics:

- the effect of nanoparticles coating the heating surface;
- the effect of nanoparticles suspended in the nano-fluids.

Accordingly, pool boiling CHF experiments were carried out by varying the wire surfaces and working fluids as summarized in Table 1.

Case 1 is pool boiling of pure water on a bare wire with smooth surface. Case 2 is pool boiling of nano-fluids on the same bare wire as case 1. The characteristics of CHF enhancement in pool boiling of nano-fluids were obtained from the results of case 2 for logarithmically different particle concentrations from $10^{-5}\%$ to $10^{-1}\%$ using both Al_2O_3 and TiO_2.

Table 1
Experimental cases of pool boiling test

Experimental case	Heater surface characteristics	Working fluid
Case 1	Bare	Pure water
Case 2	Bare	Nano-fluids
Case 3		
(a)	Nanoparticle-coated[a]	Pure water
(b)	Bare	Water used in case (a)

[a] The nanoparticle-coating on the heater surface was generated by the same procedure as the pool boiling CHF experiment of nano-fluids, but, to prevent the breakdown of the heater wire, the heat flux was only increased up to 95% of the CHF.

Case 3 estimated the effect of nanoparticles coated on the heating surface and consisted of two sub-cases. The CHF of pure water was measured on a nanoparticle-coated wire which was prepared using the same procedure as a pool boiling CHF experiment for nano-fluids on a bare wire: case 3(a). However, during the pool boiling experiment of case 3(a), nanoparticles could detach from the surface, to disperse in the fluid and effect the CHF. To check this effect, the CHF of the water used in case 3(a) was measured on a bare wire: 3(b). Finally, a comparison between the results of case 2 and 3 shows the role of nanoparticle surface coating in pool boiling CHF enhancement of nano-fluids.

2.4. Results and discussion of pool boiling experiment

2.4.1. Nano-fluids on bare wire

Prior to the experiments using nano-fluids, a number of pool boiling CHF experiments using distilled water were carried out to examine the reproducibility and repeatability of the experimental apparatus. As shown in Fig. 3, the CHF values of pure water are scattered within the analyzed uncertainty. The mean value is about 15% lower than Zuber (1959)'s prediction, which is widely used to predict the pool boiling CHF on an infinitely large flat plate:

$$\dot{q}''_{\mathrm{CHF},Z} = \frac{\pi}{24}\rho_{\mathrm{g}}^{1/4} h_{\mathrm{fg}} \sqrt[4]{g\sigma(\rho_{\mathrm{f}} - \rho_{\mathrm{g}})} \tag{4}$$

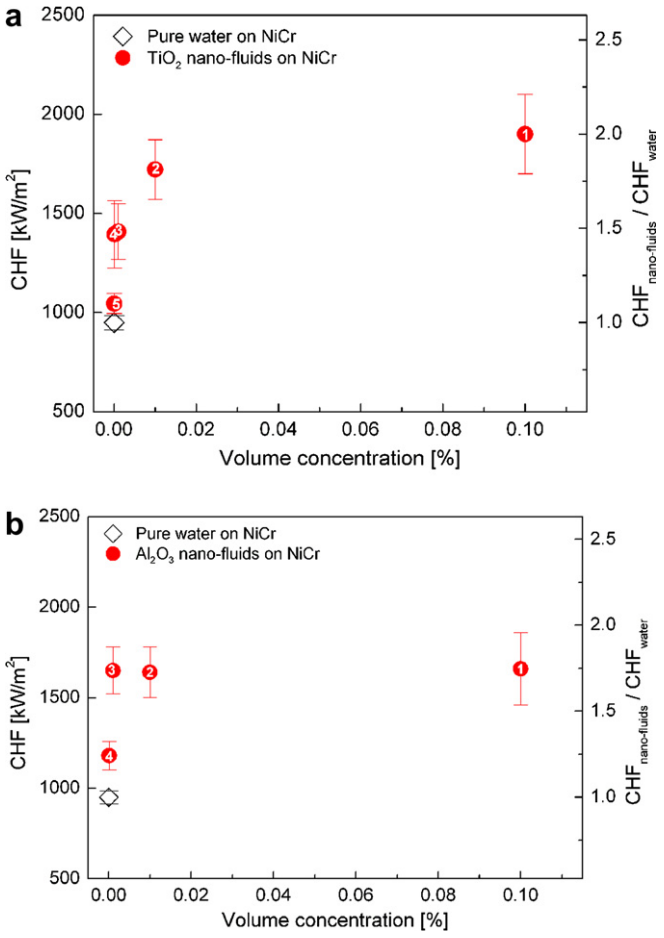

Fig. 3. Pool boiling CHF of pure water and nano-fluids: (a) TiO_2; (b) Al_2O_3.

where $\dot{q}''_{CHF,Z}$ is the CHF, ρ_g is the gas density, ρ_f is the liquid density, and h_{fg} is the latent heat for vaporization.

Barkhru and Lienhard (1972) reported that the Zuber correlation of Eq. (1) is not valid for a sufficiently small horizontal wire. The decrease of CHF on the very small wire, such as the 0.2 mm Ni–Cr wire used in this experiment, has been observed in several previous studies (Pitts and Leppert, 1966; Tachibana et al., 1996; Van Stralen and Sluyter, 1969). Therefore, the decrease of CHF in this work is consistent with general behavior. Since the main focus is to investigate CHF enhancement of nano-fluids compared to that of pure water, the CHF of pure water obtained by experiment was used as the basis for the subsequent CHF comparisons.

Fig. 3 shows pool boiling CHF values of TiO_2–water and Al_2O_3–water nano-fluids at atmospheric pressure. Both nano-fluids can achieve significant enhancements, and the degree of the enhancement is dependent on the particle volume concentration. The CHF of Al_2O_3–water nano-fluids increased to 170% of the value of pure water as the particle concentration was increased to 10^{-3}%, but changed little above that value. The CHF of TiO_2–water nano-fluids behaved similarly, reaching 180% of the pure water value at 10^{-2}% and increasing slightly at higher concentrations. The saturation phenomena of CHF enhancement observed in this work has been also shown by You et al. (2003) in pool boiling CHF experiments of water–Al_2O_3 nano-fluids at a sub-atmospheric pressure of 19.94 kPa.

Fig. 4 compares the results of this work and of previous research. At similar particle concentrations (0.1% and 0.5%), the CHF values of this work and Vassallo et al. (2004) are similar even though the material of the nanoparticles is different. The data of Bang and Chang (2005) are higher than others because the CHF of pure water in their experiment is higher than in others studies. As a result, the maximum CHF enhancements in all works on nano-fluids are about 900 kW/m^2. This shows that the result of this study is consistent with those of other works under atmospheric pressure.

2.4.2. Nanoparticle surface coating

The Ni–Cr wire surface was observed subsequent to the pool boiling CHF experiment using scanning electron microscopy (SEM) to examine the interaction between the nanoparticles and the surface. Both Al_2O_3 and TiO_2 nanoparticles were deposited on the wire surface, as shown in Figs. 5 and 6.

The cause of nanoparticle surface coating can be deduced from observation of the surface microstructures. First, the deposition structure has consistent thickness with regard to orientation, i.e., the coating on the top surface was not thicker than that on the bottom. Moreover immersion only of heating wire without heating produced only negligible coating of the wire. These facts show that the surface coatings were formed due to the nucleation, growth and departure of vapor bubbles, and not due to particle–surface interaction in a single phase or the gravitational sedimentation of nanoparticles.

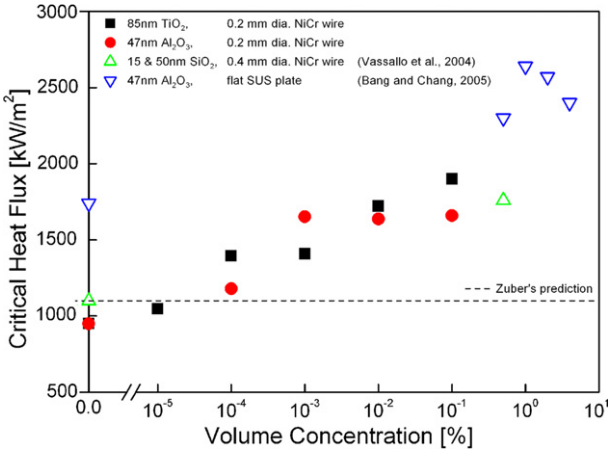

Fig. 4. Comparison of pool boiling CHF values with data from previous research.

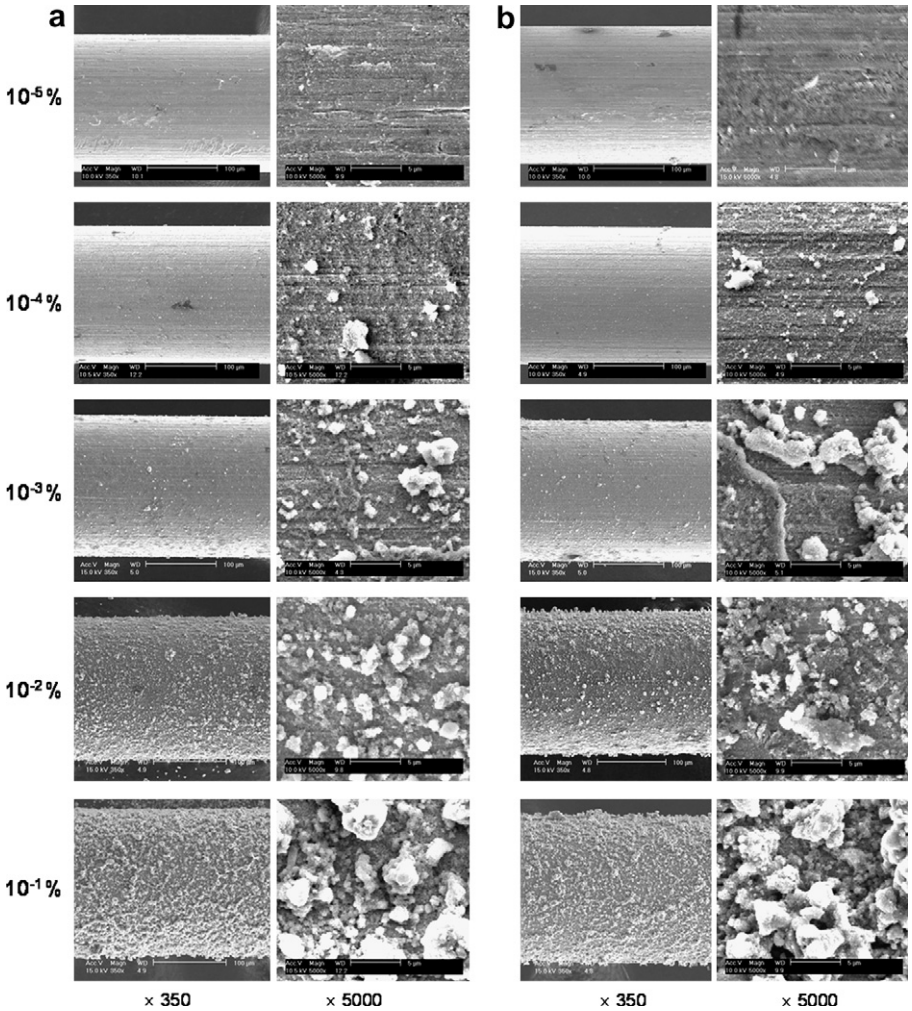

Fig. 5. SEM images of heater surfaces after pool boiling of (a) TiO_2–water nano-fluids on a bare heater and (b) pure water on TiO_2 nanoparticle-coated heaters.

The nanoparticle coating significantly changes the microscopic configuration of the wire surface. The characteristics of the nanoparticle surface coating are markedly different according to the kind of nanoparticle used. TiO_2 nano-fluids produced a rough coating formed by the deposition of the aggregated nanoparticles, and this coating was enhanced by increasing concentration. On the other hand, Al_2O_3 nano-fluids formed a relatively smooth coating with local variations in thickness. And the surface structure was fully developed at 10^{-3}% and did not change at higher concentrations.

2.4.3. Pure water on nanoparticle-coated wire

Fig. 7 shows the results of pool boiling experiments to show the effect of TiO_2 nanoparticles coated on the wire surface. The CHF of pure water on the nanoparticle-coated heater varied with the concentrations of nano-fluids used for surface coating. However, the CHFs on the bare wire immersed in water, which was used in the coated wire experiment, were similar to that of pure water on the bare wire within the estimated uncertainty. Thus, the amount of nanoparticles that can detach from the nanoparticle-coated surface during pool boiling is extremely small and their effect on CHF is also negligible. Therefore, the CHF enhancement of pure water on the nanoparticle-coated wire in Fig. 7 is due to the change of surface structure characteristics by nanoparticle coating.

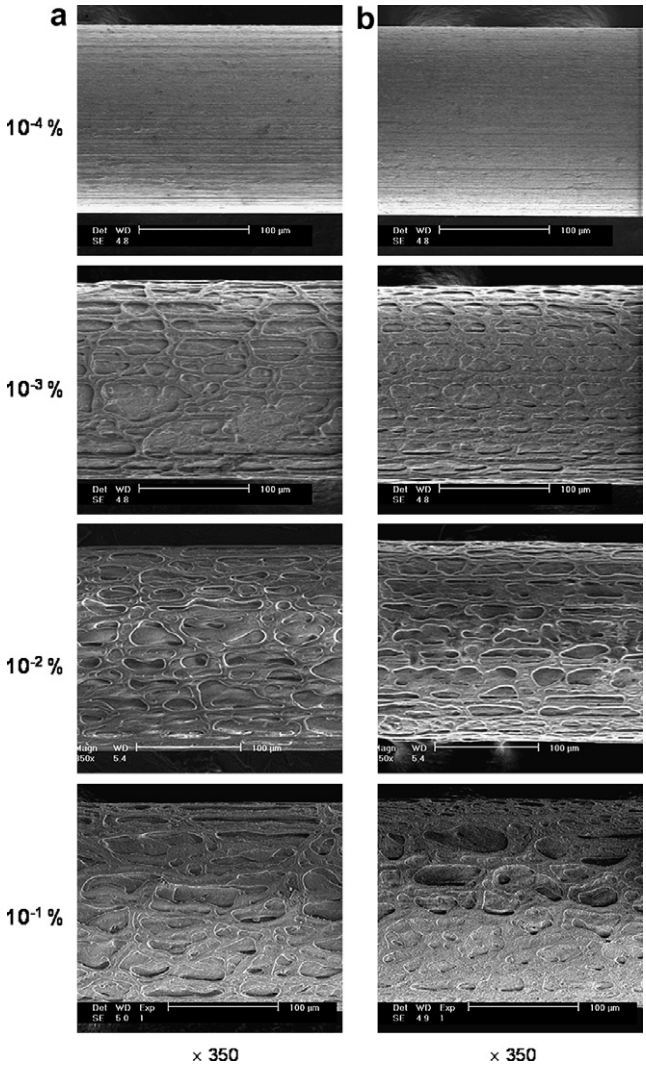

Fig. 6. SEM images of heater surfaces after pool boiling of (a) Al_2O_3–water nano-fluids on a bare heater and (b) pure water on Al_2O_3 nanoparticle-coated heaters.

Fig. 8 compares the CHF enhancement of nano-fluid on bare wire with that of pure water on the nanoparticle-coated wire. For all particle concentrations of both nano-fluids, the CHF enhancements of pure water on the nanoparticle-coated wire were at least as large as those of nano-fluids. Moreover, as shown in Figs. 5 and 6, there is no appreciable difference in the surface characteristics of the wires for two different experimental cases with the same concentrations. Thus, Fig. 8 clearly shows that the effect of nanoparticles coated on heating surface is a prime factor in the CHF enhancement of nano-fluids.

For Al_2O_3–water nano-fluids, the CHF enhancement is almost the same as that of pure water on the nanoparticle-coated wire within the uncertainty as given in Fig. 8b. On the other hand, for TiO_2–water nano-fluids, CHF enhancements of pure water on the nanoparticle-coated heater are similar to that of nano-fluids at particle concentrations below 10^{-3}%, but much higher at concentrations over 10^{-2}%, as shown in Fig. 8a. Since the characteristics of the heater surfaces are the same, the only difference was the nanoparticles suspended in the working fluid. In this regard, there is an effect of the suspended nanoparticles whereby the application of TiO_2–water nano-fluids degrades the CHF enhancement of pure water from the TiO_2 nanoparticle-coated surface.

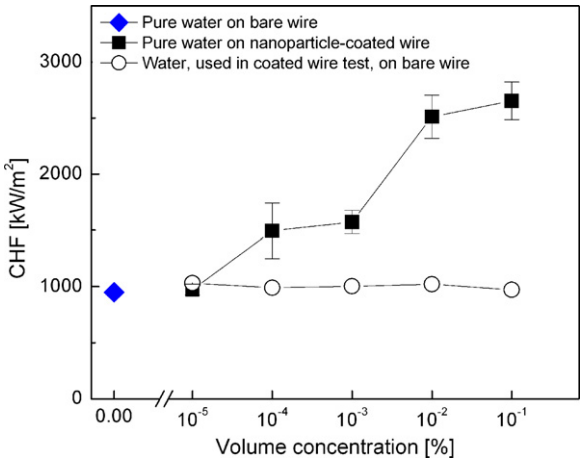

Fig. 7. CHF enhancement of pure water on a TiO_2 nanoparticle-coated heater.

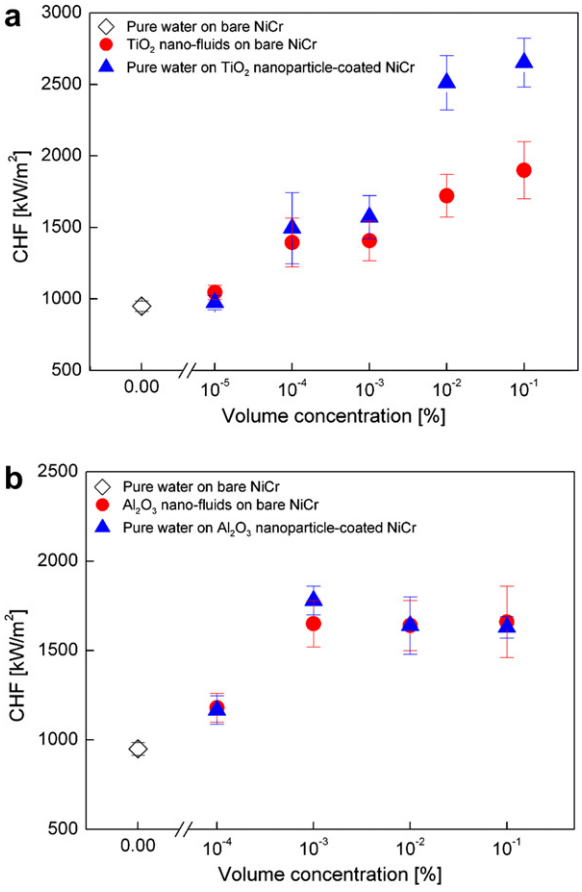

Fig. 8. Comparison of CHF enhancements of nano-fluids on a bare heater and pure water on nanoparticle-coated heaters: (a) TiO_2; (b) Al_2O_3.

3. Characterization of heater surface

The previous section has shown that the main reason of CHF enhancement of nano-fluids is the modification of the heating surface due to nanoparticle coating. Therefore, in order to understand the mechanism of

CHF enhancement using nano-fluids, it is necessary to characterize the heating surface using the parameters that can be closely related with pool boiling CHF phenomena. The parameters chosen in this work are surface roughness (R_a), contact angle (θ), and capillary wicking performance (Lc). But it is impossible to measure the surface parameters of the small diameter wire used in this study through conventional methods. Therefore, new quantitative measurement methodologies were adopted for the surface roughness and contact angle.

3.1. Surface roughness evaluation

An SEM image focused on the side edge of the wire was captured with magnification of 1200. The profile of the boundary between the wire and background was extracted by image processing software. Then, the two-dimensional profile was digitalized using the scale bar in the captured images. The digitalized profile contained about 470 points with 0.21 μm spacing along the wire. Finally, the surface roughness (R_a) of each wire was calculated using following equation (Provder and Kunz, 1996):

$$R_a = (1/l)\int_0^l |Y(X) - \overline{Y}|\,dx \approx \frac{1}{N}\sum_{i=1}^{N} |Y_i - \overline{Y}| \tag{5}$$

Here, l is the horizontal length of test wire in the captured image, X is the horizontal position, Y is the vertical height in the two-dimensional profile, and $\overline{Y}$ is the mean vertical height. However, the surface roughness of the Al_2O_3 nanoparticle-coated wire could not be estimated using this technique because of its structure (see Fig. 6).

3.2. Contact angle measurement

To measure the contact angle of a wire, the wire was horizontally mounted. A 2 μL water droplet was placed on the wire. The shape of droplet on the wire was captured using the high speed camera. The angle between the wire and the droplet boundary at the triple point was measured from the captured image.

3.3. Capillary wicking height measurement

A wire was fixed vertically and the bottom of the wire was immersed in a reservoir. Then, as the liquid in the reservoir moved up the wire, the rising liquid column was captured using a high speed camera. Using the captured images, the heights of the liquid column being moved were estimated not only at the maximum point that occurred within several seconds but also at the saturated state after several minutes.

3.4. Results and discussion of surface characterization

The surface deposition of suspended nanoparticles during pool boiling of nano-fluids significantly changes the microscopic configurations of the wire surface as shown in Figs. 5 and 6. In order to quantify the structural change of the heater surface, the surface roughness (R_a) was employed. Fig. 9 shows the values of R_a measured on the wires corresponding to the various particle concentrations of TiO_2–water nano-fluids. R_a values increased with increasing concentration. This is consistent with the results of Bang and Chang (2005), who reported that the surface roughness of test heaters submersed in Al_2O_3–water nano-fluids increased with increasing particle concentration. SEM observation of Al_2O_3 nanoparticle-coated wires given in Fig. 6 confirms the morphological enhancement of the surface. Without doubt, the change of R_a happens due to the nanoparticle surface coating. The increasing R_a indicates that the nanoparticle surface coating is not uniform and can make larger and more fractal structures as the particle concentration increases.

Many previous studies have shown the effect of surface roughness on boiling heat transfer and CHF. It has been found that the surface roughness can enhance CHF by 25–35% in general (Haramura, 1991; Nishikawa et al., 1982; Ramilison and Lienhard, 1987). However, it is not the roughness itself that affects the characteristics of nucleate boiling, but the number of active nucleation sites existing on the heating surface (Roy Chowdhury and Winterton, 1985). CHF enhancement using simple surface roughening can be attributed to increase

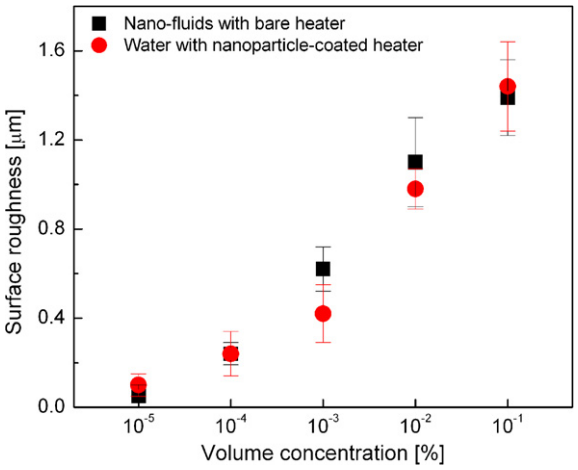

Fig. 9. Effect of TiO_2 nanoparticle surface coating on surface roughness.

of the number of active nucleation sites. But, previous research on pool boiling of nano-fluids (Bang and Chang, 2005; Das et al., 2003) have noted that the number of active nucleation sites is decreased due to the surface coating of nanoparticles. Less active nucleation on the nanoparticle-coated wire is opposed to the common phenomena of the roughened surface with CHF enhancement. From the point of view, it is hard to consider that only the effect of surface roughness (R_a) can cause the unusual CHF enhancement of the nanoparticle-coated surface.

On the other hand, the nanoparticle coating can alter not only the surface geometry but also the interfacial properties between the solid (the wire) and surrounding liquid, especially the physico-chemical properties of the surface. The surface coating of oxidized metal nanoparticles (e.g. TiO_2 or Al_2O_3) used in this work can make a roughening effect as well as oxidation on a bright metal surface. It has been reported that roughening and oxidation of metal surface can reduce the contact angle (Hong et al., 1994). Actually, the contact angles of water on the nanoparticle coated surfaces are much smaller than that of the bare wire, as shown in Fig. 10.

Roy Chowdhury and Winterton (1985) conducted a systematic investigation into the surface effect on transition boiling, and found that the contact angle (or the surface wettability) could significantly influence the transition boiling including the CHF. Takata et al. (2005) reported that the CHF of a super-hydrophilic surface is about two times as high as that of normal surface. Recently, Fukada et al. (2004) studied CHF enhancements of pure water using electrically heated Pt wire fouled with a scale deposit with high wettability. They found that a scale of a few microns thickness could induce a 167% increase in the CHF. Therefore, it can be confirmed from the results of previous studies that contact angle has a very strong influence on the pool boiling CHF. Accordingly, the considerable improvement of surface wettability in nanoparticle-coated surface may be the cause of the unusual CHF enhancement.

The other important characteristic of nanoparticle-coated surfaces is the capillary wicking performance. It is possible that the formation of microstructures due to nanoparticle surface coating induces capillary wicking on the heater surface. Fig. 11 shows the maximum capillary wicking height (Lc_{max}) on nanoparticle-coated wires. The wires prepared with particle concentrations below 10^{-4}% do not create a liquid rise due to capillary wicking, because the micro-structures of the heating surface at those concentrations are not enough to act as micro-flow-passes. Liquid rises on the wires are observed for the particle concentrations above 10^{-3}%, but the capillary wicking performances greatly differ between Al_2O_3 and TiO_2 nanoparticle-coated wires. The TiO_2 nanoparticle coated wire has an Lc_{max} of 1.2 mm at the concentration of 10^{-3}%, and then Lc_{max} steeply increases to 4.7 mm at 10^{-2}% and to 5.9 mm at 10^{-1}%. On the other hand, Al_2O_3 nanoparticle coated wire has a nominal Lc_{max} below 0.5 mm for all concentrations. This difference occurs because of the different micro-structures shown in Figs. 5 and 6.

In addition, Fig. 12 shows the effect of working fluid (pure water and nano-fluids) on the capillary wicking behavior on a TiO_2 nanoparticle-coated wire. For the same wire, the Lc_{max} of pure water is a little lager than

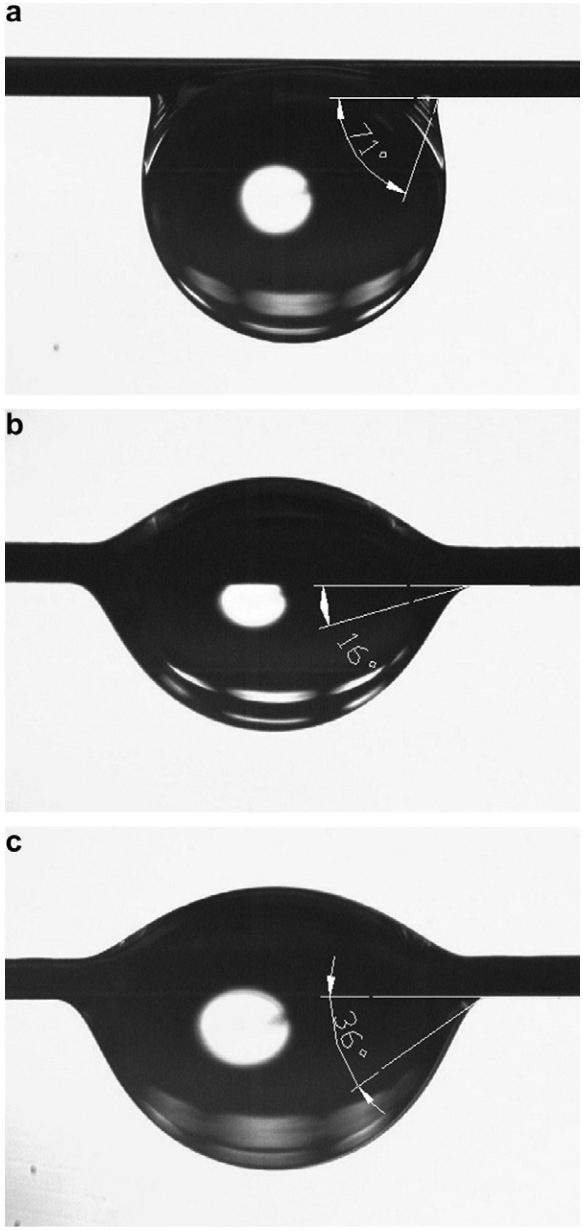

Fig. 10. Effect of nanoparticle surface coating on contact angle: (a) bare NiCr wire; (b) TiO_2 nanoparticle-coated NiCr wire (10^{-2}%); (c) Al_2O_3 nanoparticle-coated NiCr wire (10^{-1}%).

that of the nano-fluids. Furthermore, after reaching at the maximum wicking height, the capillary wicking height of pure water is maintained at that maximum value, but that of nano-fluids slowly goes down and becomes saturated at the lower wicking height. This behavior is related with whether sufficient liquid from the reservoir can be continuously supplied to maintain the wicking height or not. When evaporation occurs by natural convection from the wire to the environment, the capillary wicking height of pure water is maintained because there is a continuous flow of liquid from the reservoir to the wire. However, nano-fluids could cause clogging of micro-flow-passes due to the suspended nanoparticles. As a result, the wicking height of nano-fluids decreases as shown in Fig. 12.

The effect of a capillary porous layer on pool boiling CHF has been analyzed by Tehver (1992). His analysis was from the macrolayer concept based on Haramura and Katto (1983)'s CHF model, which considers the

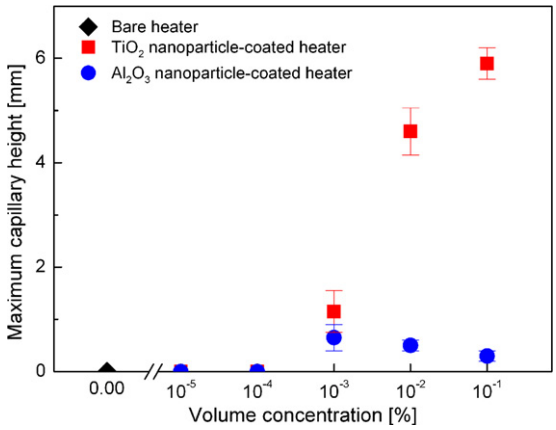

Fig. 11. Effect of nanoparticle surface coating on maximum capillary wicking height: (a) TiO_2; (b) Al_2O_3.

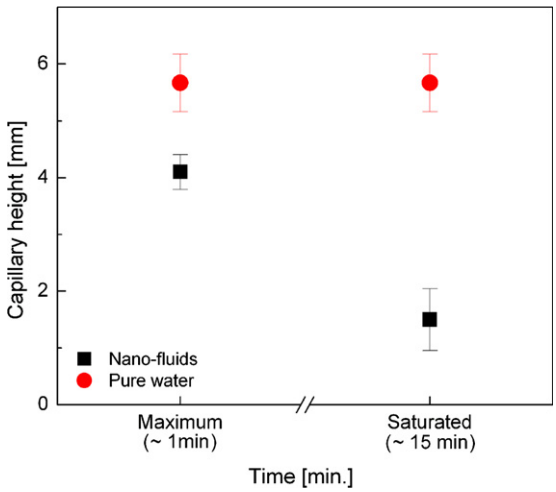

Fig. 12. Capillary wicking behaviors of pure water and TiO_2–water nano-fluids on a TiO_2 nanoparticle-coated heater. The nano-fluids concentration was 10^{-1}%, and the nanoparticle-coated heater was prepared using a 10^{-1}% nano-fluids.

formation and evaporation of a macrolayer under a bubble. He has hypothesized that the liquid suction due to capillary wicking helps to supply bulk liquid to the heating surface, so the boiling crisis can be more effectively delayed. That effect indicates that the unusual CHF enhancements on the naoparticle-coated wire in this study can be closely related to the capillary wicking performance due to the surface morphology with micro-scale structures. Considering boiling as a rapid and massive evaporation process, the clogging of micro-flow-passes by suspended nanoparticles could impede the supply of bulk liquid to the heating surface. Accordingly, CHF enhancement on nanoparticle-coated surface will be degraded if nano-fluids are used instead of pure water.

At the concentrations above 10^{-3}% having the measurable capillary wicking height, it was found that the behavior of CHF enhancement (shown in Fig. 8) corresponds well to the capillary wicking performance of nanoparticle-coated wire. CHF enhancement is very largely dependent upon capillary wicking on a heating surface (e.g. CHF of pure water on TiO_2 naoparticle-coated wire). But the wicking effect can be prevented by the clogging on micro-flow-pass due to nanoparticles suspended in working fluid, and the enhancement will be degraded (e.g. CHF of TiO_2–water nano-fluids). If capillary wicking on the wire is nominal, the difference between the CHFs of nano-fluids and of pure water on the nanoparticle-coated wire may hardly exist (e.g. CHF of pure water on Al_2O_3 nanoparticle-coated surface vs. CHF of Al_2O_3–water nano-fluids).

4. Conclusions

The conclusions drawn from this study are:

1. Nano-fluids instead of pure water as a cooling liquid significantly increased pool boiling CHF. The CHFs were enhanced at volumetric particle concentrations from 10^{-5}% to 10^{-1}%, with a maximum CHF increase of about 100%.
2. Deposition of nanoparticles on the heating surface happened during pool boiling of nano-fluids. Characteristics of nanoparticle surface coating were strongly dependent on the type and the concentration of the nanoparticle material.
3. The reason for significant CHF enhancement of nano-fluids was the surface modification due to nanoparticle coating. This is proved by the fact that CHF of nano-fluids could be reproduced using pure water on a nanoparticle-coated surface, prepared during pool boiling of nano-fluids.
4. Surface coating by oxidized metal nanoparticles during pool boiling of Al_2O_3–water and TiO_2–water nano-fluids could significantly enhance the surface wettability. The very good wetting of cooling liquid on the heating surface can largely increase CHF.
5. Fractal microstructures formed by deposition of aggregated TiO_2 nanoparticles induce liquid suction due to capillary wicking, which makes the CHF of pure water much higher than that of nano-fluids. However, the much higher CHF of the nanoparticle-coated heating surface is degraded by use of nano-fluids instead of pure water as a working fluid, since nanoparticles suspended in nano-fluids may clog micro-flow-passes supplying the bulk liquid to the heating surface by capillary wicking.

Acknowledgements

This work was supported by the Ministry of Science and Technology of Korea through the National Research Laboratory program.

References

Bang, I.C., Chang, S.H., 2005. Boiling heat transfer performance and phenomena of Al_2O_3–water nano-fluids from a plain surface in a pool. Int. J. Heat Mass Transfer 48, 2407–2419.

Barkhru, N., Lienhard, J.H., 1972. Boiling from small cylinders. Int. J. Heat Mass Transfer 15, 2011–2025.

Brinkman, H.C., 1951. The viscosity of concentrated suspension and solutions. The J. Chem. Phys. 20, 571.

Das, S.K., Putra, N., Roetzel, W., 2003. Pool boiling characteristics of nano-fluids. Int. J. Heat Mass Transfer 46, 851–862.

Fukada, Y., Haze, I., Osakabe, M., 2004. The effect of fouling on nucleate pool boiling of small wires. Heat Transfer-Asian Res. 33, 316–329.

Haramura, Y., 1991. Steady state pool transition boiling heated with condensing steam. In: Proceedings of ASME/JSME Thermal Engineering Joint Conference 2, pp. 59–64.

Haramura, Y., Katto, Y., 1983. A new hydrodynamic model of critical hear flux, applicable widely to both pool and forced convection boiling on submersed bodies in saturated liquids. Int. J. Heat Mass Transfer 26, 389–399.

Holman, J.P., 2001. Experimental Methods for Engineers, seventh ed. McGraw-Hill, New York (Chapter 3).

Hong, K.T., Imadojemu, H., Webb, R.L., 1994. Effect of oxidation and surface roughness on contact angle. Exp. Thermal fluid Sci. 8, 279–285.

Kim, H.D., Kim, J.B., Kim, M.H., 2006a. Experimental study on CHF characteristics of water–TiO_2 nano-fluids. Nucl. Eng. Technol. 38, 61–68.

Kim, S.J., Truong, B., Buongiorno, J., Hu, L.W., Bang, I.C., 2006b. Study of two-phase heat transfer in nanofluids for nuclear applications. In: Proceedings of ICAPP '06, Reno, NV USA, June 4–8.

Milinova, D., Kumar, R., 2005. Role of ions in pool boiling heat transfer of pure and silica nanofluids. Appl. Phys. Lett. 87, 233107.

Murshed, S.M.S., Leong, K.C., Yang, C., 2005. Enhanced thermal conductivity of TiO_2–water based nanofluids. Int. J. Thermal Sci. 44, 367–373.

Nishikawa, K., Fujita, Y., Ohta, H., Hidaka, S., 1982. Effects of system pressure and surface roughness on nucleate boiling heat transfer. Mem. Fac. Eng. Kyushu Univ. 42, 95–123.

Pitts, C.C., Leppert, G., 1966. The critical heat flux for electrically heated wires in saturated pool boiling. Int. J. Heat Mass Transfer 9, 365–377.

Provder, T., Kunz, B., 1996. Application of profilometry and fractal analysis to the characterization of coatings surface roughness. Prog. Org. Coat. 27, 219–226.

Ramilison, J.M., Lienhard, J.H., 1987. Transition boiling heat transfer and film transition regime. J. Heat Transfer 111, 480–486.
Roy Chowdhury, S.K., Winterton, R.H.S., 1985. Surface effects in pool boiling. Int. J. Heat Mass Transfer 28, 1881–1889.
Tachibana, F., Akiyama, M., Kawamura, H., 1996. Non-hydrodynamic aspects of pool boiling burnout. J. Nucl. Sci. Technol. 3, 121–130.
Takata, Y., Hidaka, S., Cao, J.M., Nakamura, T., Yamamoto, H., Masuda, M., Ito, M., 2005. Effect of surface wettability on boiling and evaporation. Energy 30, 209–220.
Tehver, J., 1992. Influence of porous coating on the boiling burnout heat flux. Recent Advances in Heat Transfer. In: Proceedings of the First Baltic Heat Transfer Conference, pp. 231–242.
Van Stralen, S.J.D., Sluyter, W.M., 1969. Investigations on the critical heat flux of pure liquids and mixtures under various conditions. Int. J. Heat Mass Transfer 12, 1353–1384.
Vassallo, P., Kumar, R., D'Amico, S., 2004. Pool boiling heat transfer experiments in silica–water nano-fluids. Int. J. Heat Mass Transfer 47, 407–411.
Wen, D., Ding, Y., 2005. Experimental investigation into the pool boiling heat transfer of aqueous based γ-alumina nanofluids. J. Nanoparticle Res. 7, 265–274.
You, S.M., Kim, J.H., Kim, K.H., 2003. Effect of nanoparticles on critical heat flux of water in pool boiling heat transfer. Appl. Phys. Lett. 83, 3374–3376.
Zuber, N., 1959. Hydrodynamic aspects of boiling heat transfer. AEC Rep. AECU-4439.